Anode/Cathode Geometry and Shielding Gas Interrelationships in GTAW

Electrode tip geometry and groove geometry must be compatible to ensure arc stability

BY J. F. KEY

ABSTRACT. A comprehensive set of experiments to determine specific effects of tungsten electrode tip geometry and shielding gas compositions (consisting of pure argon, pure helium, five mixtures of argon and helium, and one mixture of argon and hydrogen) on penetration was conducted. Performance of various combinations of tip geometry and shielding gas in three common weld groove geometries was assessed.

No optimum electrode tip geometry or shielding gas composition was found for all GTAW conditions. Penetration increased with electrode vertex angle when welding on flat plate. Helium additions generally increased penetration.

Electrode tip geometry and groove geometry must be compatible to ensure arc stability. Conclusions are based on heat transfer models that are heavily dependent on tungsten electrode vertex angle and shielding gas thermophysical properties.

Introduction

Early work by Savage et *al.*[1] and Chihoski[2,3] on penetration effects of tungsten electrode (cathode) tip geometry in autogenous gas tungsten arc welding (GTAW) was put in perspective by Spiller and MacGregor[4] who differentiated between partial penetration welds on thick plate and full penetration welds on thin plate. A study limited to Alloy 600 has been presented more recently by Glickstein et *al.*[5] Various heat transfer models[6-15] have been presented to rationalize these results. These works were generally concerned with arcs shielded by inert, pure gases, usually argon.

Since many GTAW procedures call for shielding gas mixtures of argon and helium or argon and hydrogen as well as edge preparations whose geometry varies for the joint, the interrelationships between shielding gas composition and electrode geometry (both anode and cathode) need to be assessed. This task was initiated to provide this assessment, and, as such, is part of a larger program to fully characterize fusion welds from heat source through unaffected base material.

Experimental Procedure

All materials used were from the same heat of 12.7 mm (0.5 in.) thick AISI Type 304 stainless steel plate. For anode geometry studies, standard 75 deg V grooves, 40 deg U grooves [4.76 mm (0.188 in.) root radius], and 10 deg narrow grooves [2.5 mm (0.10 in.) root face extension] were machined into the plate.

A solid-state, series-regulated 150 A GTAW power supply was used as the current source. A precision positioner driven by a stepping motor was utilized to move the specimen under a fixed torch. Two-percent thoriated tungsten electrodes, 2.38 mm (0.094 in.) in diameter, and custom, premixed shielding gases were used. Argon-helium compositions were 10, 25, 50, 75, and 90 vol-% helium, with the balance argon. A 95 vol-% argon-5 vol-% hydrogen mixture also was evaluated. Ultra-high purity argon and helium were used as pure, unmixed shielding gases.

Paper presented at the 61st AWS Annual Meeting held in Los Angeles, California, during April 13-18, 1980.

J. F. KEY is Scientist, Materials Engineering Branch, Fuels and Materials Division, EG&G Idaho, Inc., Idaho Falls, Idaho.

Partial penetration (≃30% of plate thickness) single spot welds and constant current bead welds were made on flat plates and in grooves to encompass a wide range of welding methods. The spot welds represented overlapping spot welds produced using high current-short duration current pulsations. Spot welds were 2.0 s in duration, and bead-on-plate welds were made at 3.0 mm/s (7.09 ipm). An arc gap of 1.00 mm (0.039 in.) was used with pure argon but had to be increased as helium was added. Pure helium required a gap of 1.50 mm (0.059 in.).

High-speed cinematography was used to analyze arc dynamics and arc interactions with the groove. A 16-mm rotating prism camera was used to film all welds with the exception of the bead-in-groove welds (in which groove walls obscured a lateral view of the arc). A camera speed of 500 frames/s was adequate for the purposes of this study. Neutral density filters were used to attenuate arc intensity. Timing light marks on film (Eastman Kodak MS 2256 color instrumentation film) edges allowed quantification of temporal events. (See Reynolds and Key[16] for more details.) Films were viewed using a motion analysis projector.

Table 1 gives the experimental matrix of weld types produced as a function of electrode tip geometry and shielding gas composition. All welds were sectioned and prepared for metallographic examination. Macrophotographs were taken of each section. Fusion zone depth, width, and area were measured on the flat plate welds. Only the fusion zone area was measured on groove welds since fiducial reference marks needed for depth measurements were destroyed during welding.

Results

Figure 1 shows arc shape and resulting fusion zone profile as a function of electrode tip geometry for stationary spot-on-plate welds. Note that the arc changes from a "bell" shape at small vertex angles to a more constricted "ball" shape at large vertex angles. Also, the arc is uniformly more constricted for the larger truncation diameter, 0.500 mm (0.020 in.).

Macrophotographs of the fusion zone show a corresponding shape change. As the arc becomes more constricted, the fusion zone becomes narrower and much deeper. These fusion zone dimensions are reasonably constant at vertex angles over 90 deg. Figure 2 shows a graphical plot of these results and corresponding bead-on-plate welds (only the depth/width ratio need be plotted since it reflects trends in depth, width, and area); the correlation coefficient, r^2, only applies to the 15-90 deg portion of the plot. In subsequent plots, r^2 will apply to the entire plot.

Figure 3 shows the effect of helium and hydrogen additions to argon

Table 1—Experimental Matrix

Vertex angle and truncation diameter, deg/mm	Shielding gas composition, vol-%							
	100 Ar	90 Ar/10 He	75 Ar/25 He	50 Ar/50 He	25 Ar/75 He	10 Ar/90 He	100 He	95 Ar/5 H_2
15/0.125	SOP,[a] BOP[b]							
/0.500	SOP, BOP							
30/0.125	SOP, BOP SIG,[c] BIG[d]	SOP, BOP SIG, BIG	SOP, BOP SIG, BIG	SOP, BOP SIG, BIG	SOP, BOP SIG, BIG	SOP, BOP SIG, BIG	SOP, BOP SIG, BIG	SOP, BOP SIG, BIG
/0.500	SOP, BOP							
45/0.125	SOP, BOP							
/0.500	SOP, BOP							
60/0.125	SOP, BOP SIG, BIG	SOP, BOP SIG, BIG	SOP, BOP SIG, BIG	SOP, BOP SIG, BIG	SOP, BOP SIG, BIG	SOP, BOP SIG, BIG	SOP, BOP SIG, BIG	SOP, BOP SIG, BIG
/0.500	SOP, BOP							
75/0.125	SOP, BOP							
/0.500	SOP, BOP							
90/0.125	SOP, BOP							
/0.500	SOP, BOP SIG, BIG	SOP, BOP SIG, BIG	SOP, BOP SIG, BIG	SOP, BOP SIG, BIG	SOP, BOP SIG, BIG	SOP, BOP SIG, BIG	SOP, BOP SIG, BIG	SOP, BOP SIG, BIG
120/0.125	SOP, BOP							
/0.500	SOP, BOP							
180	SOP, BOP	SOP, BOP	SOP, BOP	SOP, BOP	SOP, BOP	SOP, BOP	SOP, BOP	SOP, BOP

[a]Spot-on-plate (2.0 s).
[b]Bead-on-plate (3.0 mm/s).
[c]Spot-in-groove (75 V-groove, 40 U-groove, 10 narrow groove), 2.0 s.
[d]Bead-in-groove (75 V-groove, 40 U-groove, 10 narrow groove), 3.0 mm/s.

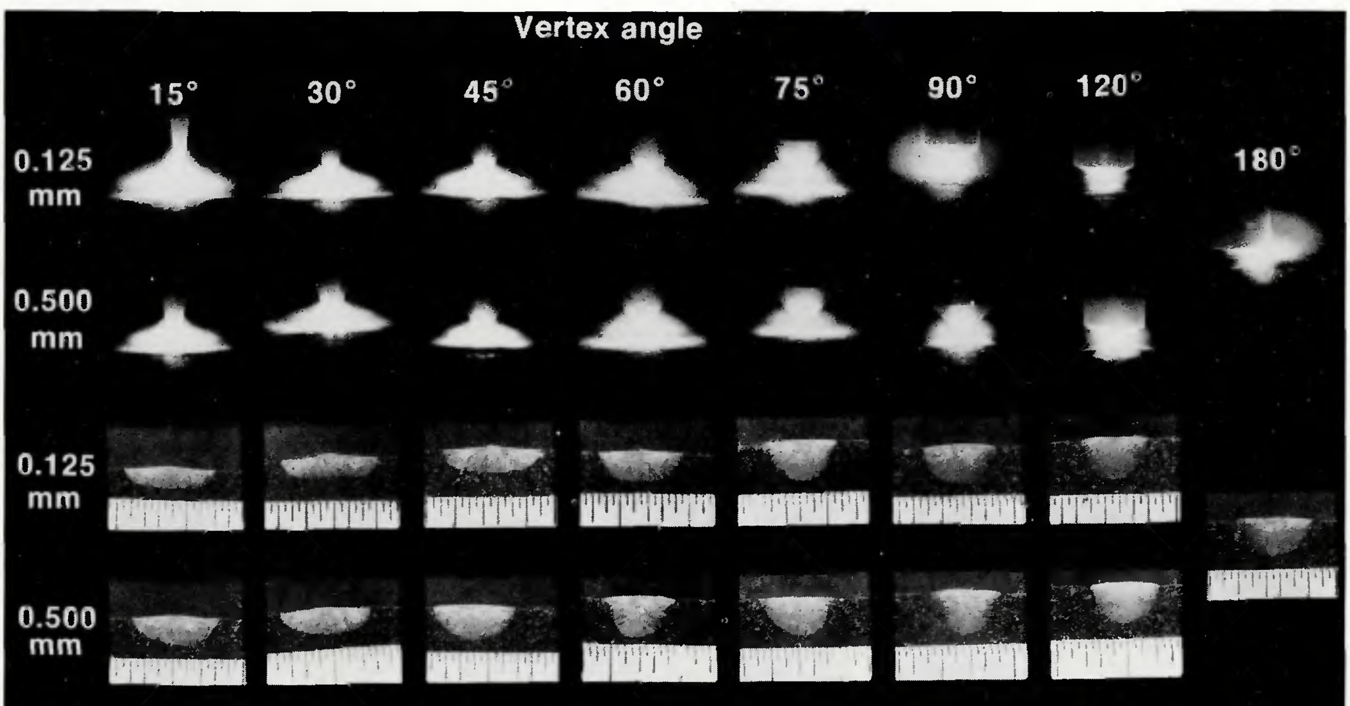

Fig. 1—Arc shape and fusion zone profile as a function of electrode tip geometry in a pure argon shield (150 A, 2.0 s spot-on-plate)

shielding gas on fusion zone profile in spot-on-plate welds. Figure 4A shows graphical results of depth/width as a function of helium content for spot-on-plate welds. As expected, helium additions cause a large increase in penetration (273%) when using an electrode with a sharp tip geometry such as a 30 deg vertex angle with 0.125 mm (0.005 in.) diameter truncation. A significant increase (148%) is obtained for a moderate 60 deg tip. However, electrodes with blunt 90 or 180 deg vertex angles produced only slightly improved penetration (22 and 8%, respectively) when helium was added.

For these particular welding conditions, helium has little benefit if a blunt tip geometry is used. The poor correlation coefficient for the 180 deg plot and, to a lesser extent, the 90 deg plot is attributed to arc instability. Arcs were generally less stable for blunt electrodes than sharp ones regardless of shielding gas composition. Arcs from a 180 deg tip geometry are very unstable unless the weld is made at the electrode's maximum current limit to ensure uniform emission from the entire tip.

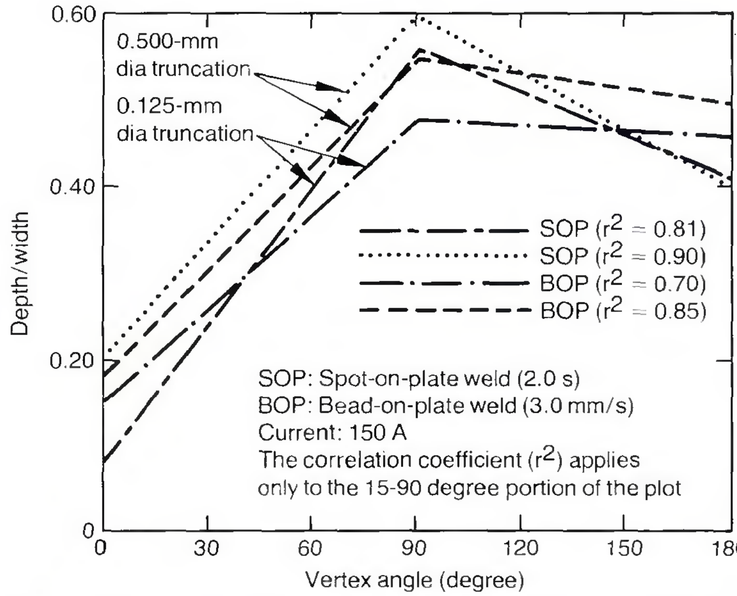

Fig. 2—Fusion zone depth/width as a function of electrode tip geometry in a pure argon shield (150 A, 2.0 s spot-on-plate and 3.0 mm/s bead-on-plate)

Effects of helium and hydrogen additions to argon were sought for bead-on-plate welds. These welds were made at a fairly rapid 3.0 mm/s (7.09 ipm) rate. Figure 4B shows results which differ somewhat from corresponding spot-on-plate welds. All electrode tip geometries performed similarly to the 90 deg electrode in spot-on-plate welds, where the penetration is somewhat greater, but the influence of helium and the amount of scatter, reflected in r^2, is similar. However, Larson[17] reports results from bead-on-plate welds made at slower travel speeds $\simeq$1.0 mm/s (2.36 ipm) that are similar to spot-on-plate results in Figs. 3 and 4A. Obviously, welding speed effect on molten pool geometry is responsible for these differences. Figure 5 shows variations in depth/width due to electrode vertex angle in a 95 Ar-5H_2 shield for both spot-on-plate and bead-on-plate welds. Although the depth/width is uniformly greater at all vertex angles, the trends are the same as for a pure argon shield—Fig. 2.

Figure 6 shows the fusion zone area as a function of helium content and electrode tip geometry for spot-in-groove welds. Figure 6A is for a 75 deg V groove, Fig. 6B is for a 40 deg U groove, and Fig. 6C is for a 10 deg narrow groove. Although helium has a moderate to significant effect on fusion zone area in both the V-groove and U-groove, it generally has less effect in the narrow groove. In general, the sharper electrode tip geometries produce larger fusion zone areas.

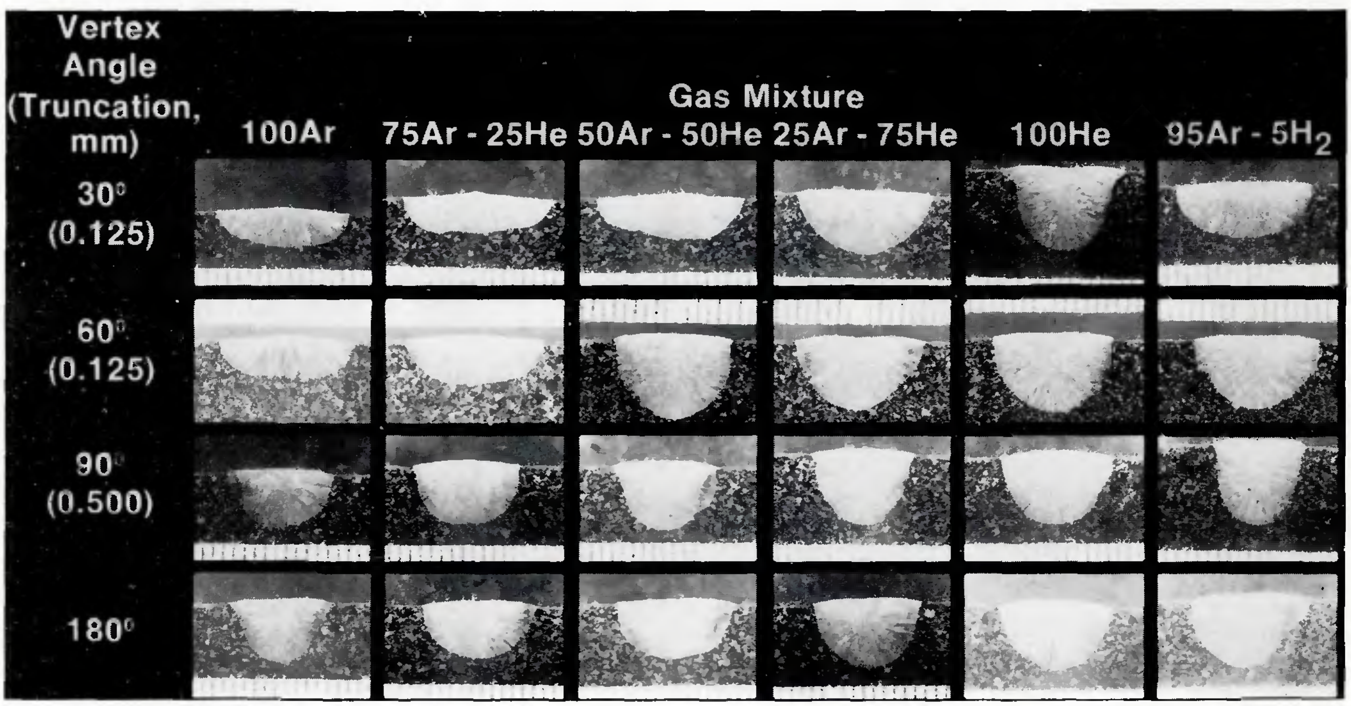

Fig. 3—Fusion zone profile as a function of electrode tip geometry and helium or hydrogen content of shielding gas (150 A, 2.0 s spot-on-plate).

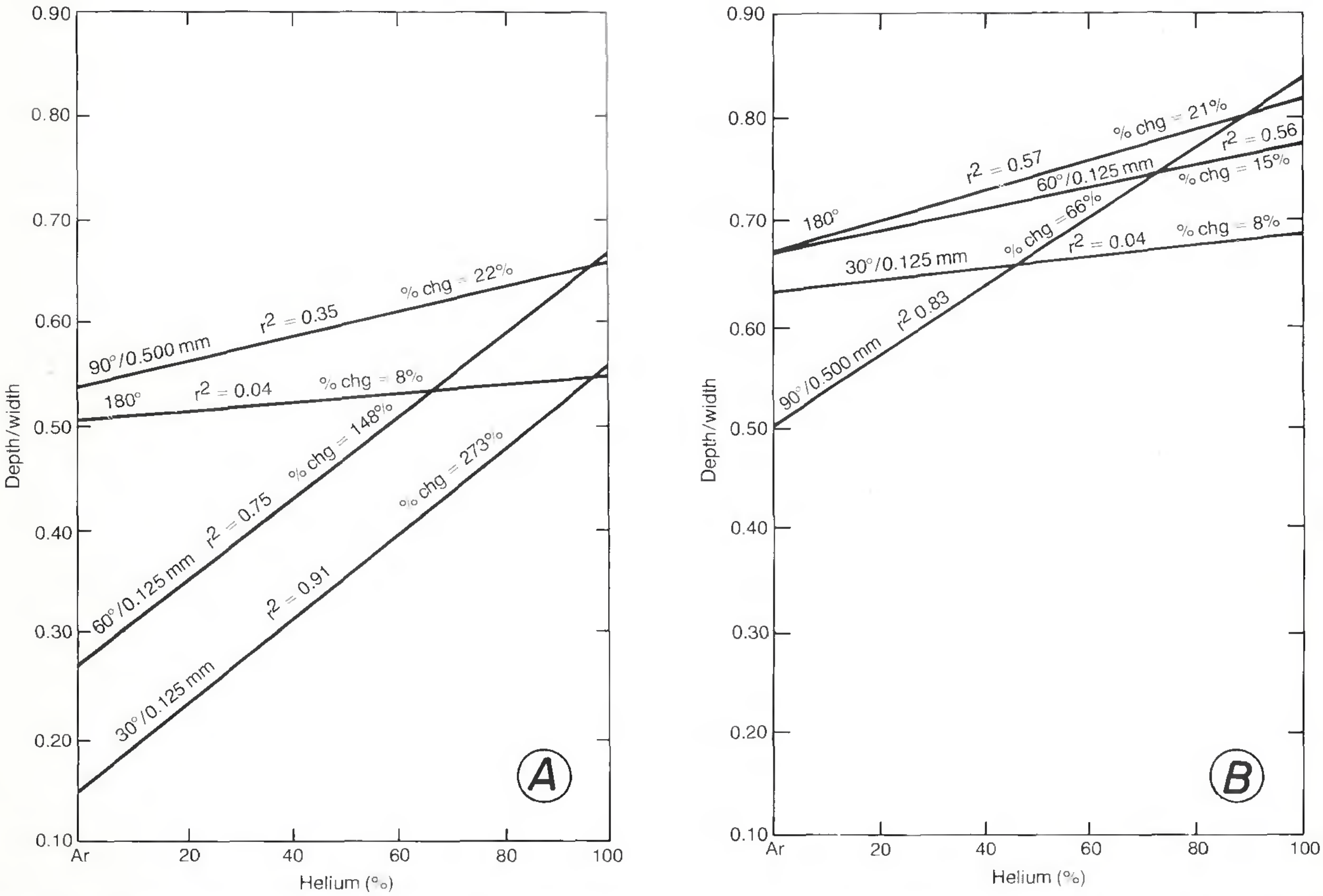

Fig. 4—Fusion zone depth/width as a function of electrode tip geometry and helium content of the shielding gas at 150 A: A—2.0 s spot-on-plate; B—3.0 mm/s bead-on-plate

Figure 7 shows corresponding bead-in-groove welds, which indicate that helium additions are much more effective for increasing fusion zone area in bead-in-groove than for spot-in-groove welds. Although electrode tip geometry has little effect on fusion zone area in pure argon, the sharp geometries are clearly superior in high helium-content shielding gases. Figure 8 shows the dependence of the fusion zone area on electrode vertex angle in a 95 Ar-5H_2 shield for both spot-in-groove and bead-in-groove welds.

A limited number of experiments were repeated to provide an indication of the statistical validity of results. For spot-on-plate experiments, errors in depth/width were less than 10% for "sharp," e.g., 30 deg electrode tip geometries, and up to 25% for "blunt," e.g., 90 deg electrode tip geometries. Decreased arc stability for blunt electrodes may account for the increased variation. For bead-on-plate experiments, errors in depth/width fell within a 10% variation for all electrode tip geometries.

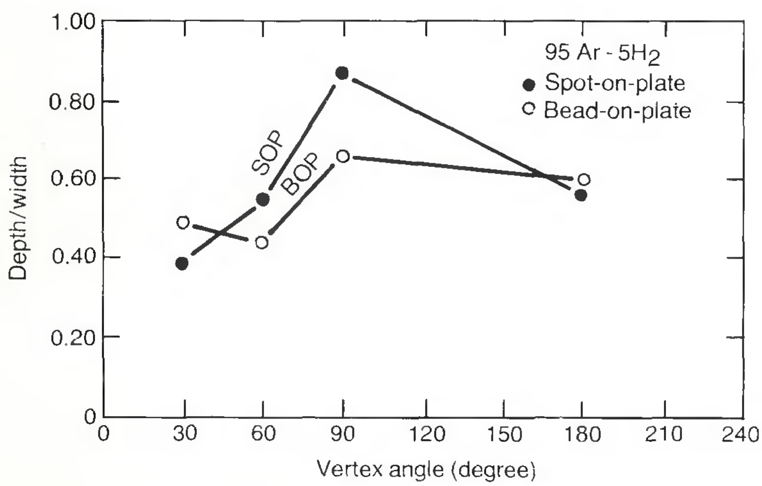

Fig. 5—Fusion zone depth/width as a function of electrode tip geometry in a 95 argon-5 hydrogen volume percent shielding gas for both spot-on-plate (150 A, 2.0 s) and bead-on-plate (150 A, 3.0 mm/s) welds.

Discussion

Spot-on-plate and bead-on-plate results from this investigation and arc temperature measurements[18] for the same combinations of electrode tip geometry and shielding gas composition support heat transfer models that depend, in part, on electrode tip geometry and thermophysical properties of the shielding gas. Shaw[6] characterizes an arc produced by an electrode with a small vertex angle as a line heat source that is poorly distributed. Temperatures would be high along the axis but much lower elsewhere. Conversely, an electrode with a large vertex angle produces a distributed heat source which is much more efficient in producing deep penetration welds. Ludwig[8] found that high thermal conductivity gases such as helium and hydrogen (at certain temperatures) produce a uniformly distributed heat source regardless of the electrode tip

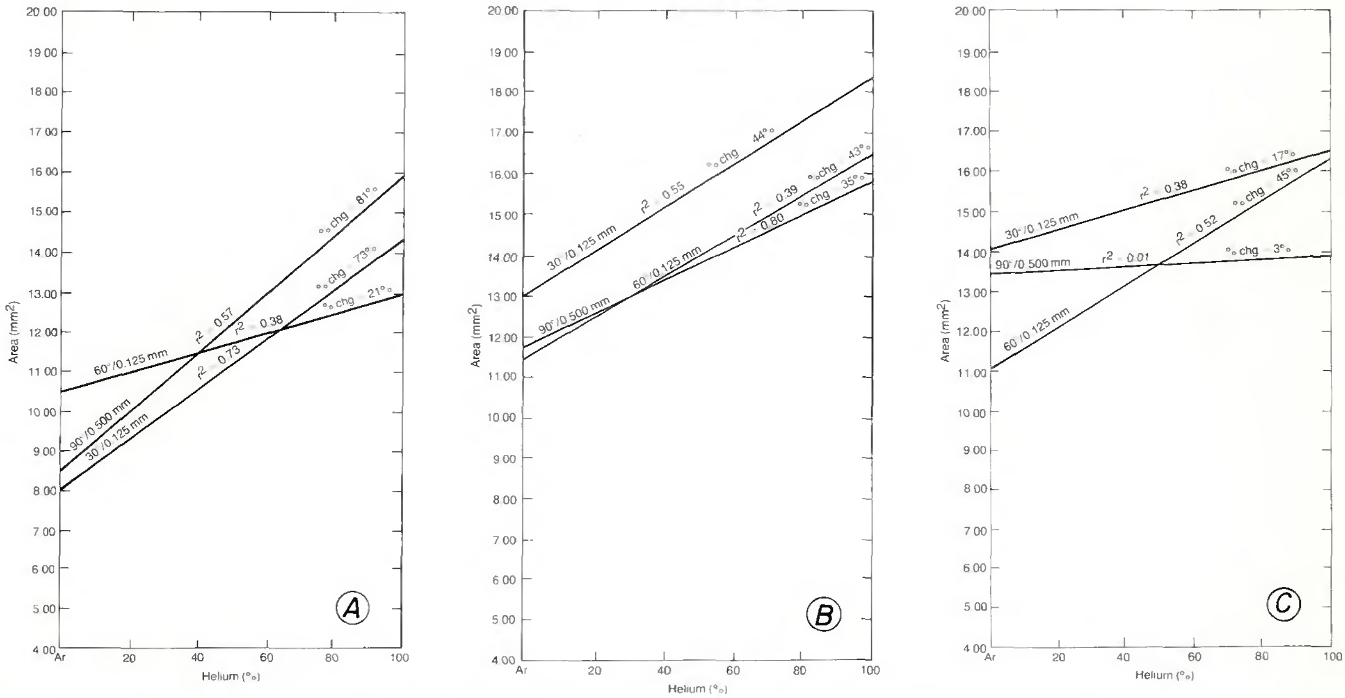

Fig. 6—Fusion zone area as a function of electrode tip geometry and helium content of the shielding gas for 150 A, 2.0 s spot-in-groove welds: A—75 deg V groove; B—40 deg U-groove; C—10 deg narrow groove

geometry. The high thermal conductivity and specific heat of helium and hydrogen (compared to argon) also aid in transferring more heat to the anode.

Results were compared to previously published data—Table 2.[1,4,5] Trends in data were similar to Savage *et al.*[1] and Spiller *et al.*[4] with the following exceptions: a maximum in fusion zone depth and a minimum in width occurred for electrode vertex angles in the 75 to 90 deg range. Savage's[1] data showed a uniform increase in depth and decrease in width up to 180 degrees. Spiller's[4] data showed the opposite trend, i.e., a slight decrease in depth with increasing vertex angles, but a similar trend to Savage's[1] data in width. It should be noted that Savage used carbon steel and Spiller used Type 321 stainless steel.

Savage found no dependence of fusion zone area on electrode vertex angle. Present results for spot-on-plate welds show that the area increases uniformly with vertex angle. However, scatter in the data for bead-on-plate results do not reflect this trend. Glickstein's[5] results for alloy 600 were considerably different. His work showed a maximum in depth, width, depth/width, and area for electrode vertex angles between 30 and 45 deg.

Two arguments are proposed to

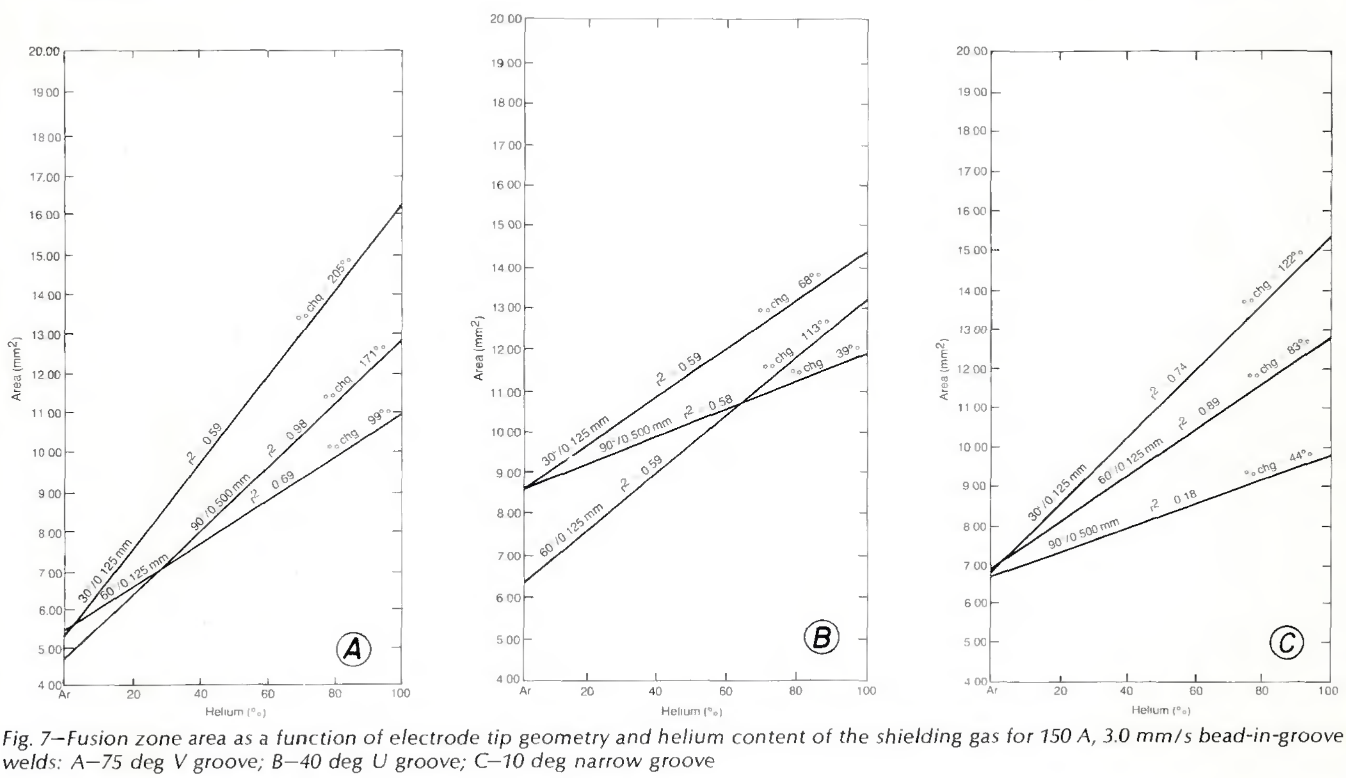

Fig. 7—Fusion zone area as a function of electrode tip geometry and helium content of the shielding gas for 150 A, 3.0 mm/s bead-in-groove welds: A—75 deg V groove; B—40 deg U groove; C—10 deg narrow groove

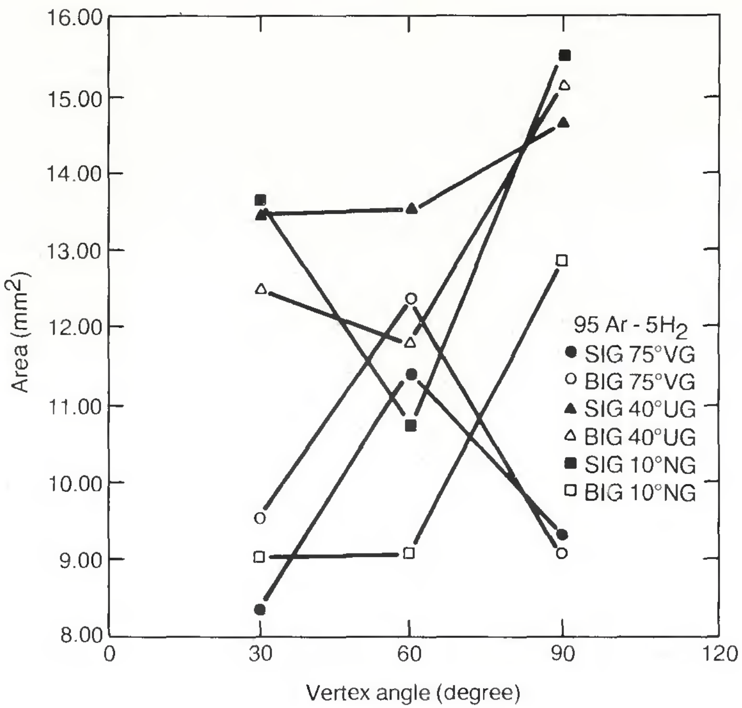

Fig. 8—Fusion zone area as a function of electrode tip geometry in a 95 argon −5 hydrogen volume percent shielding gas for both spot-in-groove (150 A, 2.0 s) and bead-in-groove (150 A, 3.0 mm/s) welds

explain these seemingly contradictory results. First, there is an obvious difference in materials being welded. Mills[19] has suggested that even trace amounts of aluminum may significantly decrease penetration. Glickstein used alloy 600 which had 0.16 wt-% aluminum, significantly more than a trace amount, whereas Savage used ASTM A 285 steel which only had 0.013 wt-% aluminum. Second, Glickstein used a welding current of 90 A, whereas these data and the data given for Savage and Spiller were produced with a current of 150 A.

It is well known that higher currents cause an arc to spread. This phenomena is much more evident in the case of a sharp electrode tip geometry, e.g., 30 deg, than for a blunt, e.g., 90 deg geometry. Therefore, differences in penetration due to electrode tip geometry should be more evident at higher welding currents.

When an arc is used to weld in a groove, other considerations must be addressed, e.g., ensuring that the shortest path to electrical ground is between the tip of the electrode and the groove bottom (or the desired location of the weld bead). A companion consideration is the relative difference in the axial temperature gradient of the electrode. Emission from the shoulder (producing an unstable arc) is more likely with a blunt electrode than a sharp one since the shoulder of the blunt electrode is at a higher temperature.

Figure 9 shows possible combinations of electrode tip geometry and groove geometry used in this investigation. Sharp electrode tip geometries, e.g., 30 deg vertex angle and a relative-

Table 2—Comparison of Results[(a),(b),(c),(d)]

Vertex angle, deg (0.125-mm diameter truncation)	Depth, mm						Width, mm						Area, mm²					
	Key		Savage[1]	Spiller[1]	Glickstein[5]		Key		Savage	Spiller	Glickstein		Key		Savage	Spiller	Glickstein	
	SOP[(e)]	BOP[(f)]	BOP	BOP	SOP	BOP	SOP	BOP	BOP	BOP	SOP	BOP	SOP	BOP	BOP	BOP	SOP	BOP
15	1.33	1.83	–	–	0.81	0.97	6.55	6.51	–	–	6.45	4.70	7.94	10.32	–	–	5.87	3.42
30	1.25	1.40	1.78	2.79	1.07	1.09	6.92	6.91	6.60	6.60	6.76	5.33	9.35	9.23	9.65	–	6.45	4.52
45	1.60	1.70	2.03	–	1.12	1.02	6.95	6.91	6.10	–	6.86	5.03	10.32	10.45	9.65	–	6.65	4.06
60	2.12	2.14	2.29	2.54	0.81	0.97	6.06	6.02	5.59	5.84	6.40	4.95	10.77	7.35	9.65	–	5.74	4.00
75	2.68	2.96	–	–	–	–	5.05	5.53	–	–	–	–	10.90	13.55	9.65	–	–	–
90	2.81	2.51	2.54	2.54	0.71	0.89	4.93	5.51	5.08	5.59	5.33	4.32	10.90	11.10	9.65	–	4.32	3.29
120	2.65	2.79	2.79	2.41	–	–	5.08	4.82	4.32	5.33	–	–	11.23	11.42	9.65	–	–	–
180	2.58	2.53	–	–	0.76	0.76	5.69	4.92	–	–	5.49	4.32	11.81	10.26	9.65	–	4.52	2.97
													$\bar{a}$ = 10.46					

(a) Savage's parameters: 150 A, 1.27 mm/s; 1.27 mm gap; carbon steel.
(b) Spiller's parameters: 150 A, 2.54 mm/s; 1.40 mm gap; Type 321 stainless steel.
(c) Glickstein's parameters: 90 A, SOP 10 s, BOP 2.12 mm/s; 0.89 mm gap; Alloy 600.
(d) Key's parameters: 150 A, SOP 2.0 s, BOP 3.0 mm/s; 1.00 mm gap; Type 304 stainless steel.
(e) Spot-on-plate.
(f) Bead-on-plate.

ly small truncation, produce the most stable arcs, especially in V groove and narrow groove welds. This may account, in part, for their equal or superior performance compared to blunt geometries. Although U grooves accept most electrode tip geometries, they are too large for economical mechanized welding.

The groove geometry has an additional effect on heat transfer to the anode. Since groove walls confine the arc and limit radiation and convection losses to the environment, electrode tip geometry has less effect on penetration. This is especially true in the case of narrow-groove joints with nearly vertical walls. The overriding consideration appears to be arc stability which indicates use of a moderately sharp electrode tip geometry (30-60 deg vertex angle).

Conclusions

Results indicate the following conclusions on anode/cathode geometry and shielding gas interrelationships in autogenous, partial-penetration GTAW:

1. Penetration increases as the tungsten electrode tip is made more blunt (15-90 deg) for both spot-on-plate and bead-on-plate welds.

2. Optimum electrode tip geometry is governed by arc stability when welding in a groove for both spot-on-plate and bead-on-plate welds. Path length to ground must be considered. Sharp tip geometries (30-60 deg) are preferred.

3. Helium and hydrogen have a beneficial effect on penetration for both spot-on-plate and bead-on-plate welds. The effect is especially strong in helium mixtures for sharp electrode tip geometries. A special case arises for spot-on-plate welds in which blunt electrode tip geometries are quite effective in pure argon.

4. Helium also has a beneficial effect on penetration when welding in a groove for both spot and bead welds.

5. Data favor heat transfer models that depend, in part, on electrode tip geometry and thermophysical properties of the shielding gas. These parameters affect both distribution and transfer of heat to the anode with resulting strong effects on fusion zone profile.

6. No optimum combination of electrode tip geometry or shielding gas composition was found for all GTAW conditions.

Acknowledgments

Appreciation is extended to L. D. Reynolds for his contributions in equipment design and fabrication and for performing high-speed cinematography and welding.

This work was supported by the U. S. Department of Energy, Assistant Secretary for Research and Development, Office of Basic Energy Sciences, under DOE Contract No. DE-AC07-76ID01570.

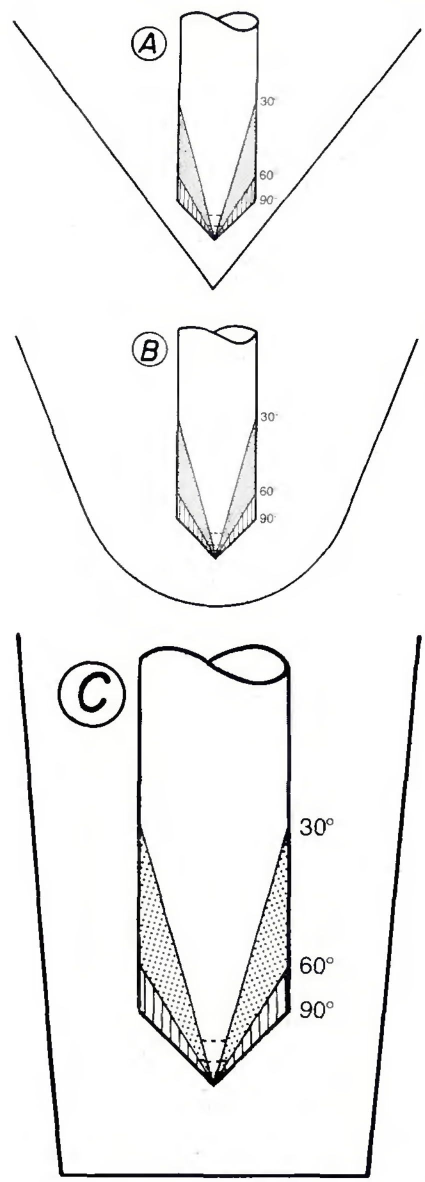

Fig. 9—Influence of electrode tip geometry and groove geometry on path length to ground: A—75 deg V groove; B—40 deg U groove; C—10 deg narrow groove

References

1. Savage, W. F., Strunck, S. S., and Ishikawa, Y., "The Effect of Electrode Geometry in Gas Tungsten-Arc Welding," *Welding Journal, 44* (11), Nov. 1965, Research Suppl., pp. 489-s to 496-s.

2. Chihoski, R. A., "The Effects of Varying Electrode Shape on Arc, Operations, and Quality of Welds in 2014-T6 Aluminum," *Welding Journal, 47* (5), May 1968, Research Suppl. pp. 210-s to 222-s.

3. Chihoski, R. A., "The Rationing of Power Between the Gas Tungsten Arc and Electrode," *Welding Journal, 49* (2), Feb. 1970, Research Suppl., pp. 69-s to 82-s.

4. Spiller, K. R., and MacGregor, G. J., "Effect of Electrode Vertex Angle on Fused Weld Geometry in TIG-Welding," *Proceedings of the Conference on Advances in Weld Processes, the Welding Institute, Abington Hall, Cambridge, UK, April 14-16, 1970,* pp. 82 to 88.

5. Glickstein, S. S., Friedman, E., and Yeniscavich, W., "Investigation of Alloy 600 Welding Parameters," *Welding Journal, 54* (4), 1975, May Research Suppl., pp. 113-s to 122-s (see Table 2).

6. Shaw, Jr., C. B., "Diagnostic Studies of the GTAW Arc," *Welding Journal, 54* (3), March 1975, Research Suppl., pp. 81-s to 86-s.

7. Quigley, M. B. C., *et al.*, "Heat Flow to the Workpiece from a TIG Welding Arc," *J. Phys. D: Appl. Phys., 6,* 1973, pp. 2250 to 2258.

8. Ludwig, H. C., "Plasma-Energy Transfer in Gas-Shielded Welding Arcs," *Welding Journal, 38* (7), July 1959, Research Suppl., pp. 296-s to 300-s.

9. Ludwig, H. C., "Current Density and Anode Spot Size in the Gas Tungsten Arc," *Welding Journal, 47* (5), May 1968, Research Suppl., pp. 234-s to 240-s.

10. Cobine, J. D., and Burger, E. E., "Analysis of Electrode Phenomena in the High-Current Arc," *J. Appl. Phys., 26,* 7, 1955, pp. 895 to 900.

11. Wilkinson, J. B., and Milner, D. R., "Heat Transfer from Arcs," *British Welding Journal, 7,* 1960, pp. 115 to 128.

12. Nestor O. H., "Heat Intensity and Current Density Distributions at the Anode of High Current, Inert Gas Arcs," *J. Appl. Phys., 33,* 1962, pp. 1638 to 1648.

13. Eckert, E. R. G., and Pfender, E., "Plasma Energy Transfer to a Surface With and Without Electric Current," *Welding Journal,* 46 (10), Oct. 1967, Research Suppl., pp. 471-s to 480-s.

14. Lancaster, J. F., "Energy Distribution in Argon-Shielded Welding Arcs," *British Welding Journal, 1,* 1954, pp. 412 to 426.

15. Jackson, C. E., and Shrubsall, A. E., "Energy Distribution in Electric Welding," *Welding Journal, 29* (5), May 1950, Research Suppl., pp. 231-s to 241-s.

16. Reynolds, L. D., and Key, J. F., *High-Speed Cinematography of Gas Tungsten Arc Welding—Theory and Applications,* EG&G-FM-5051, in preparation.

17. Larson, R. A., private communication, EG&G Idaho, Inc., March 12, 1980.

18. Key, J. F., McIlwain, M. E., and Isaacson, L., "A Plasma Diagnostics Approach to Welding Heat Source/Molten Pool Interaction," presented at *IEE Sixth International Conference on "Gas Discharges and their Applications," Heriot-Watt University, Edinburgh, UK, September 8-11, 1980.*

19. Bennett, W. S., and Mills, G. S., "GTA Weldability Studies on High Manganese Stainless Steel," *Welding Journal, 53* (12), Dec. 1974, Research Suppl., pp. 548-s to 553-s.